Hindawi
International Journal of Antennas and Propagation
Volume 2018, Article ID 9685029, 7 pages
https://doi.org/10.1155/2018/9685029

Research Article

Design of a Compact UWB MIMO Antenna without Decoupling Structure

Yanjie Wu,[1] **Kang Ding**,[2] **Bing Zhang**,[3] **Jianfeng Li**,[1] **Duolong Wu**,[1] **and Kun Wang**[4]

[1]*School of Physics and Optoelectronic Engineering, Guangdong University of Technology, Guangzhou 510006, China*
[2]*National Key Laboratory on Electromagnetic Environmental Effects and Electro-optical Engineering, PLA University of Science and Technology, Nanjing 210007, China*
[3]*College of Electronics and Information Engineering, Sichuan University, Chengdu 610064, China*
[4]*School of Information Engineering, Guangdong University of Technology, Guangzhou 510006, China*

Correspondence should be addressed to Yanjie Wu; wuyanjie@gdut.edu.cn

Received 27 September 2017; Revised 13 February 2018; Accepted 22 February 2018; Published 26 April 2018

Academic Editor: Shih Yuan Chen

A compact high isolation ultrawideband (UWB) multiple-input-multiple-output (MIMO) antenna is designed. The proposed MIMO antenna consists of a rectangular monopole antenna and a slot antenna fed by two microstrip lines, respectively. To improve the impedance matching, a circular coupling structure is designed to feed the tapered slot antenna. The parasitic resonance introduced by the ground stub helps to extend the impedance bandwidth of monopole antenna at the upper UWB band. Commonly used complex decoupling or coupling structures are eliminated that endow the proposed antenna minimized foot print, which is preferred in mobile handset. Although without decoupling structure, high isolation is obtained between two antenna elements. Simulation and measurement verify the antenna's desirable performance, showing a broad impedance bandwidth of 3.1–10.6 GHz with $|S_{11}| < -10$ dB and $|S_{21}| < -20$ dB over 3.4–10.6 GHz, and $|S_{21}| < -18$ dB from 3.1–3.4 GHz.

1. Introduction

Wireless communication systems rely on ultrawideband (UWB) and multi-input-multi-output (MIMO) technologies for high-speed data streaming [1]. Multiple antennas are employed in MIMO systems to overcome multipath fading, to improve channel capacity, and to ensure link quality [2].

As important devices of UWB MIMO systems, MIMO antennas have been investigated widely in recent years. Various decoupling structures were used to improve isolation, which is an important parameter of MIMO antennas. A compact UWB MIMO antenna with dual band-notched 3.30–3.70 GHz and 5.15–5.85 GHz was reported in [3]. Several metal strips and perturb ground plane, as decoupling structure, lead to good isolation. In [4], a couple of slots are etched on the ground plane to improve the isolation of the antennas. In [5], inverted L-shaped branches and a polygon slot function as the decoupling structure to control mutual coupling. Two inverted C-shaped ground metal strips are placed between the two radiating elements to achieve high isolation [6]. A protruded ground plane was used in [7] to improve the isolation of the MIMO antenna. Instead of introducing decoupling structure, a coupling element was introduced to enhance the isolation between two antennas in [8]. Though the abovementioned decoupling and coupling structures show their effectiveness in isolation improvement, the enlarged foot print is not preferred in a mobile handset.

A compact UWB MIMO antenna with polarization diversity was proposed in [9], with a size of $25 \times 40\,\text{mm}^2$. The minimized foot print is obtained at the cost of narrowed bandwidth. Moreover, the two antenna elements did not have a common ground plane, which makes it difficult to be used in practice. Dual-orthogonal polarization was used in [10] for high isolation, but it requires a complex feed network to excite the two polarizations. A diversity UWB antenna was proposed in [11] with limited bandwidth. In

[12], polarization diversity was also used to improve the isolation, but antenna has a large size. A carbon black film was used in [13] to improve the isolation of two antenna elements, but it will increase the cost of systems.

A UWB MIMO antenna with high isolation and compact size is presented in this paper. The proposed MIMO antenna is composed of a monopole antenna and a slot antenna. A ground stub introduces parasitic resonance that helps to extend the antenna's impedance bandwidth at the upper UWB band. Good isolation is achieved without additional coupling or decoupling structures. The proposed antenna features impedance bandwidth 3.1–10.6 GHz. The mutual coupling is less than −18 dB from 3.1–3.4 GHz and less than −20 dB from 3.4–10.6 GHz.

2. Antenna Design

2.1. Geometry of UWB MIMO Antenna. The geometry of the proposed UWB MIMO antenna is shown in Figure 1. The slot antenna and the rectangular monopole antenna, denoted as element 1 and element 2, respectively, are fed by two 50 Ω microstrip lines. Element 1 consists of two tapered stepped slots. Element 2 is a monopole antenna. The microstrip feeding lines and the monopole are on the top of the substrate and the ground plane and the slot antenna are on the bottom. Port 1 and port 2 are located at the opposite flank of the substrate which helps improve the isolation. Both two elements are designed of functional bandwidth from 3.1 to 10.6 GHz. Dimensions of the antenna are $25 \times 35 \times 0.8\ \text{mm}^3$. FR4 ($\varepsilon_r = 4.4$) is used as substrate.

As for a monopole, the gap between the radiator and the ground plane is a dominant factor on its impedance bandwidth. Besides tuning this gap, we add a parasitic stub between the monopole and slot antenna for bandwidth extension. For the initial monopole antenna structure, the fundamental resonant frequency can be calculated by [14]

$$f_r = \frac{14.4}{l_1 + l_2 + g + \left(A_1/2\pi l_1\sqrt{\varepsilon_{re}}\right) + \left(A_2/2\pi l_2\sqrt{\varepsilon_{re}}\right)}\ \text{GHz}, \quad (1)$$

where l_1 and l_2 are the length of the ground plane and the monopole antenna patch and g is the gap between them. A_1 and A_2 are the area of the ground plane and monopole antenna patch. l_1, l_2, and g are in centimetres. $\varepsilon_{re} = (\varepsilon_r + 1)/2$ is the effective dielectric constant.

The slot antenna is designed based on [15, 16]. A linear tapered slot combined with stepped slot as a radiator and a microstrip to slot transition also help to achieve the desirable bandwidth of the slot antenna.

The design values of the antenna parameters are as follows: $w_1 = 4.5$ mm, $w_2 = 1.6$ mm, $w_3 = 4.9$ mm, $w_4 = 5$ mm, $w_5 = 7.4$ mm, $w_s = 0.3$ mm, $w_7 = 1$ mm, $w_8 = 11$ mm, $w_9 = 1.6$ mm, $w_{10} = 8.4$ mm, $w_{11} = 2.27$ mm, $w_{12} = 1.86$ mm, $w_{13} = 3.54$ mm, $L_1 = 8$ mm, $L_2 = 13$ mm, $L_3 = 14$ mm, $L_4 = 12$ mm, $L_5 = 15.4$ mm, $L_6 = 1$ mm, $L_7 = 0.34$ mm, $L_8 = 1.5$ mm, $L_9 = 10$ mm, $L_{10} = 2.66$ mm, $L_{11} = 5$ mm, $R_1 = 1.9$ mm, $R_2 = 1.5$ mm, $L_s = 5$ mm, $w = 35$ mm, $L = 25$ mm, and $g = 1$ mm. The photographs of the antenna are shown in Figure 2.

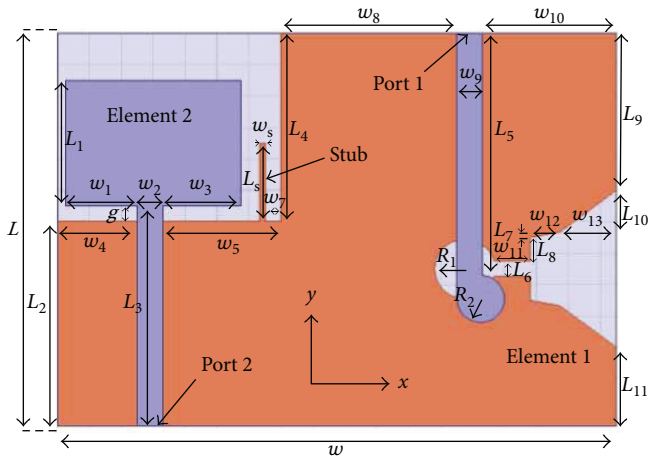

Figure 1: Design view of the proposed UWB MIMO antenna (orange: bottom side; purple: top side).

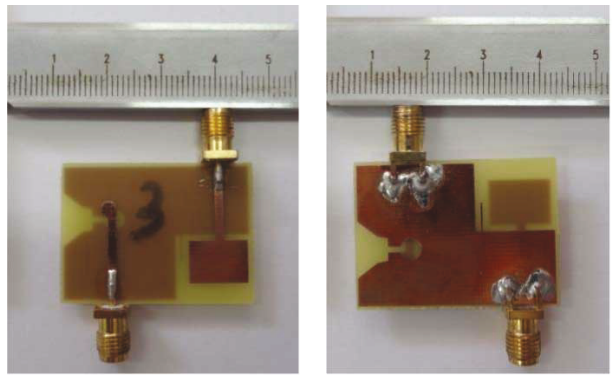

(a) (b)

Figure 2: Photographs of fabricated antenna. (a) Top view. (b) Bottom view.

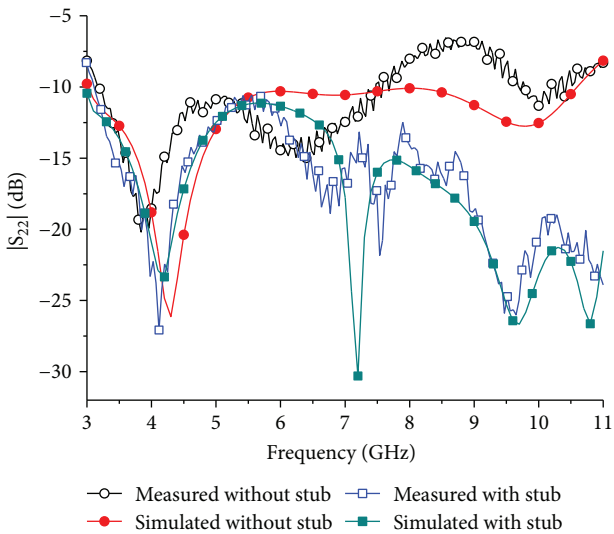

Figure 3: Simulated and measured $|S_{22}|$ of antenna with and without stub.

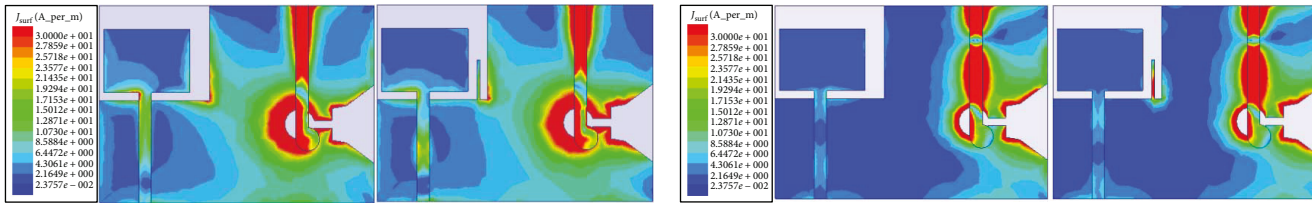

FIGURE 4: Current distribution with and without stub. (a) $f = 3.5$ GHz. (b) $f = 9$ GHz.

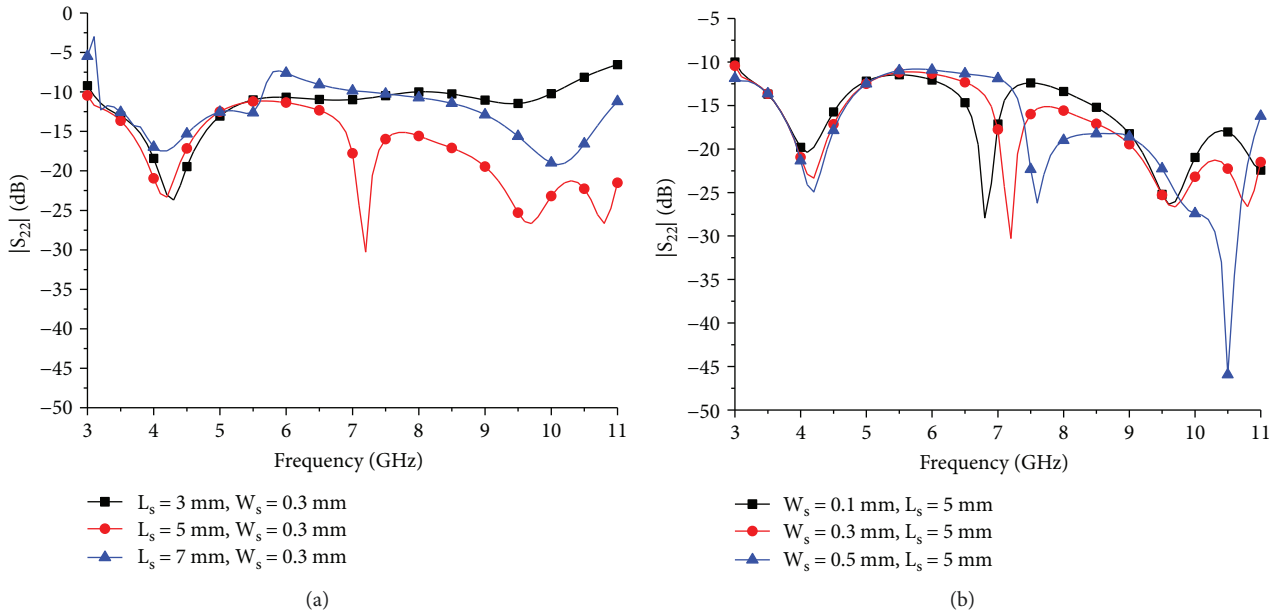

FIGURE 5: Simulated $|S_{22}|$ of the antenna with (a) different *Ls* and (b) different *Ws*.

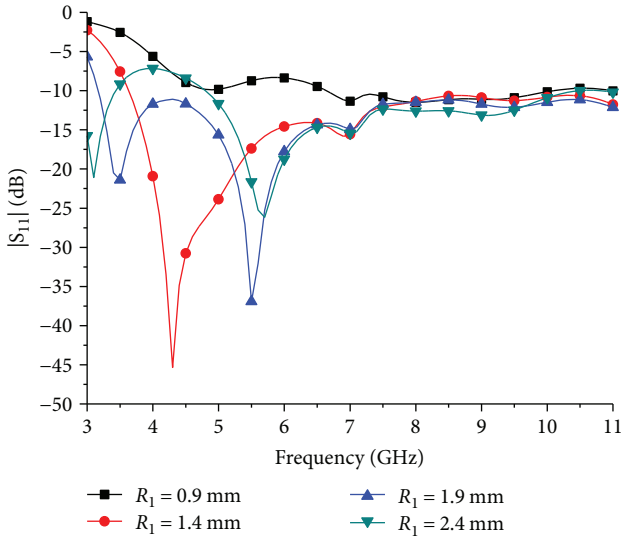

FIGURE 6: Simulated $|S_{11}|$ with different values of *R*1.

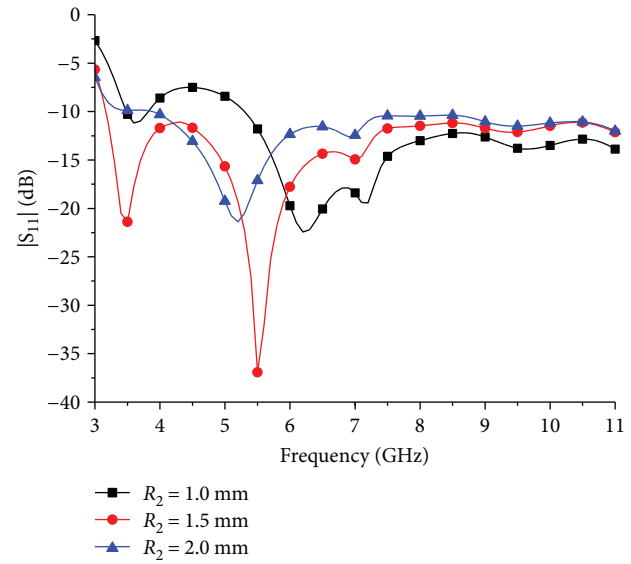

FIGURE 7: Simulated $|S_{11}|$ with different values of *R*2.

2.2. Effects of the Parasitic Stub. The influence of the parasitic stub on the antenna's input impedance is analysed in Figure 3. It shows that the stub extend the impedance of element 2 toward the upper band. That is because of the multiple parasitic resonances brought about by the stub from 6 GHz to 11 GHz. The fundamental resonance of

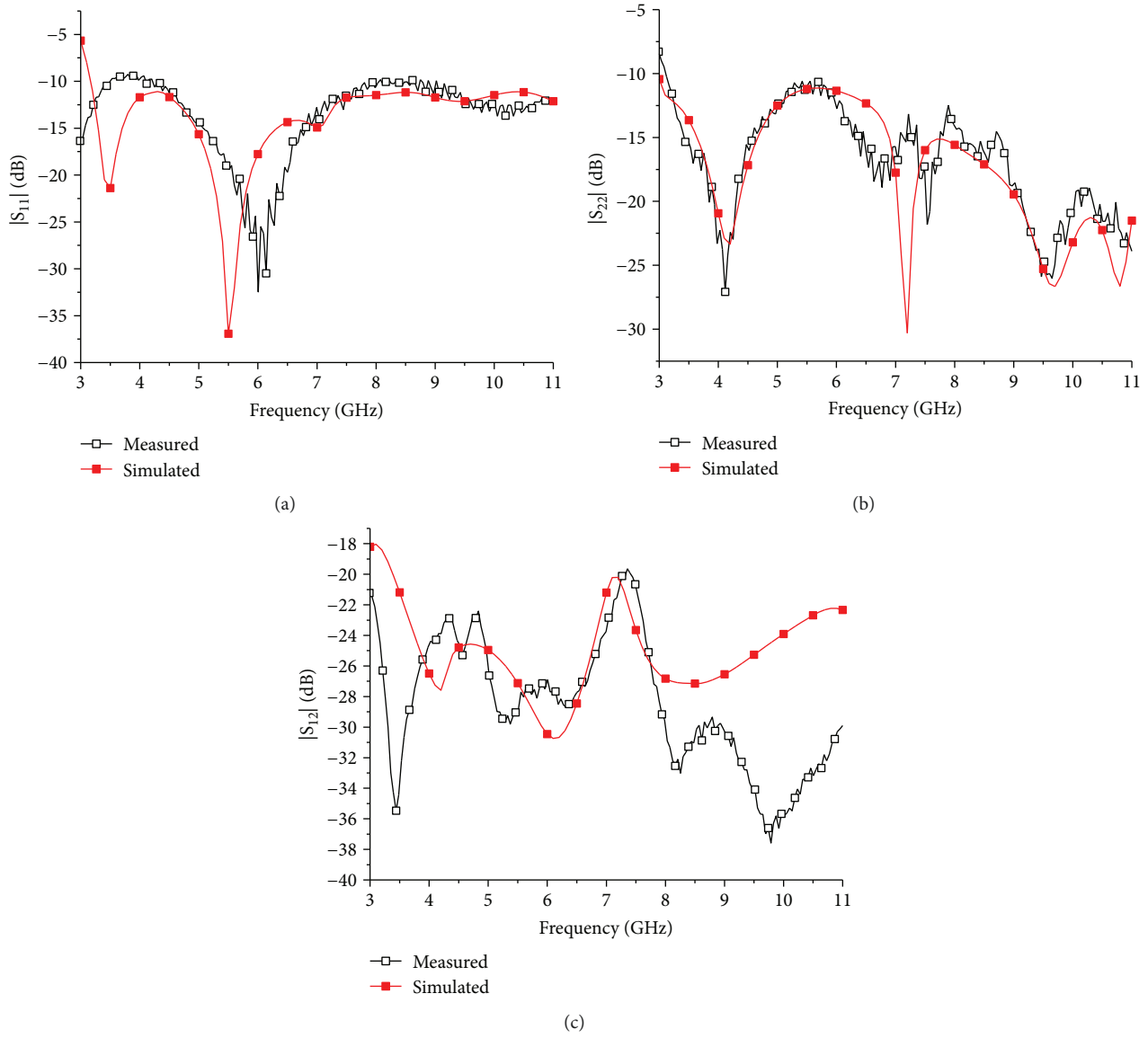

FIGURE 8: Simulated and measured S-parameters of the proposed antenna. (a) $|S_{11}|$. (b) $|S_{22}|$. (c) $|S_{12}|$.

the monopole at 4 GHz is not much affected by the parasitic stub.

Moreover, current distributions of the MIMO antennas with and without the stub in Figure 4, indicating the performance of the proposed antenna at low frequency, are not affected by the stub. For example, as shown in Figure 4(a), the current distribution of the antenna at 3.5 GHz is stable. At 9 GHz, intense current is observed on the stub in Figure 4(b), which proves the resonance brought about by the stub at the upper UWB band.

Figure 5 shows the simulated $|S_{22}|$ of the MIMO antenna with varying L_s (length of stub) and W_s (width of stub). After the parameter optimization, L_s is chosen to be 5 mm. As shown in Figure 5(a), when increasing or decreasing L_s, the $|S_{22}|$ became deteriorated for upper UWB frequencies. In Figure 5(b), $|S_{22}|$ varies dramatically from 5 GHz to 11 GHz with different W_s. W_s is chosen to be 0.3 mm for a slightly broader impedance bandwidth.

2.3. Parameter Study of R_1 and R_2. The coupling between the feeding structures is influential on the antenna's impedance bandwidth. The proposed slot antenna is fed by coupling a circular patch (radius R_1) with a circular slot (radius R_2). The effects of variations in different R_1 and R_2 are shown in Figures 6 and 7.

Figure 6 shows the slot's reflection coefficient against different R_1. When R_1 is increased from 0.9 mm to 2.4 mm, the $|S_{11}|$ curve is nearly unaffected from 7.5 GHz to 11 GHz. Two parasitic resonances appear at 3.5 and 5.5 GHz when R_1 is 1.9 mm. When R_1 is 1.4 mm, the two parasitic resonances merge into one, resulting in a narrow bandwidth. If R1 increases to 2.4 mm, the two resonances diverge toward the lower and upper side of the UWB band, and then a notch band of 3.7–5 GHz appears. In order to cover UWB band, R_1 is chosen to be 1.9 mm.

R_2 is the other influential parameter, as shown in Figure 7. It is found that the impedance bandwidth of the antenna is

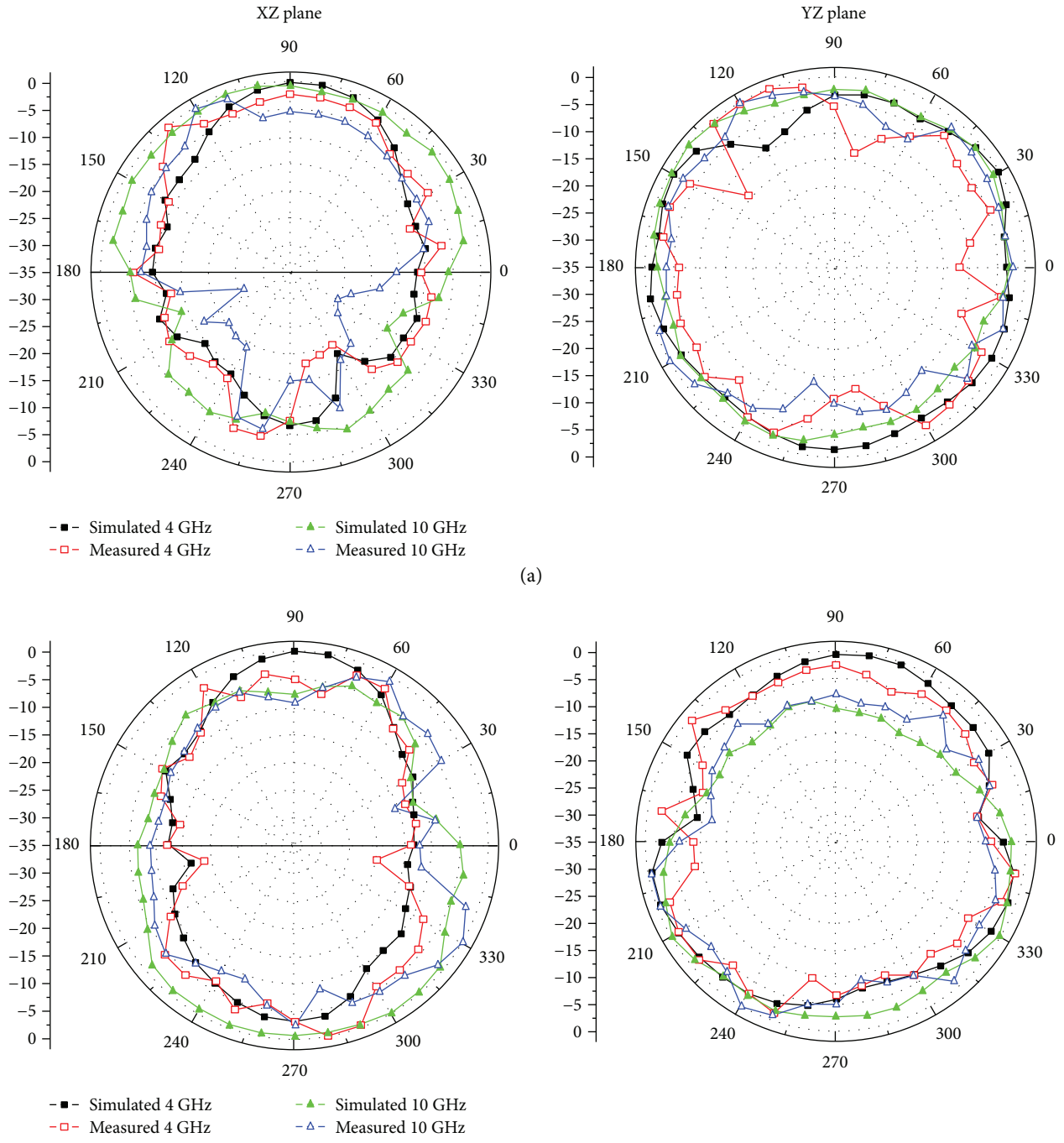

Figure 9: Simulated and measured 2D radiation patterns. (a) Port 1 is excited. (b) Port 2 is excited.

stable versus R_2 from 8–11 GHz, except for resonance at the lower side band. Different values of R_1 and R_2 lead to varying coupling coefficient, which changes the impedance matching of element 1. Finally, R_2 is chosen to be 1.5 mm.

3. Results and Discussions

3.1. Impedance Bandwidth. The antenna is simulated by the full-wave electromagnetic High Frequency Structure Simulator (HFSS) and measured with an Agilent E5071C network analyser. The simulated and measured $|S_{11}|$, $|S_{22}|$, and $|S_{12}|$ of the proposed antenna are shown in Figure 8. Figures 8(a) and 8(b) show the proposed UWB MIMO antenna has an impedance bandwidth with $|S_{11}| < -10$ dB from 3.1 GHz to more than 11 GHz. As shown in Figure 8(c), the mutual coupling (in terms of $|S_{12}|$) is below −18 dB for 3.1–3.4 GHz and below −20 dB over 3.4–10.6 GHz. In general, the simulated and measured results are in good agreement. Discrepancies between measured and simulated results come principally from fabrication tolerances.

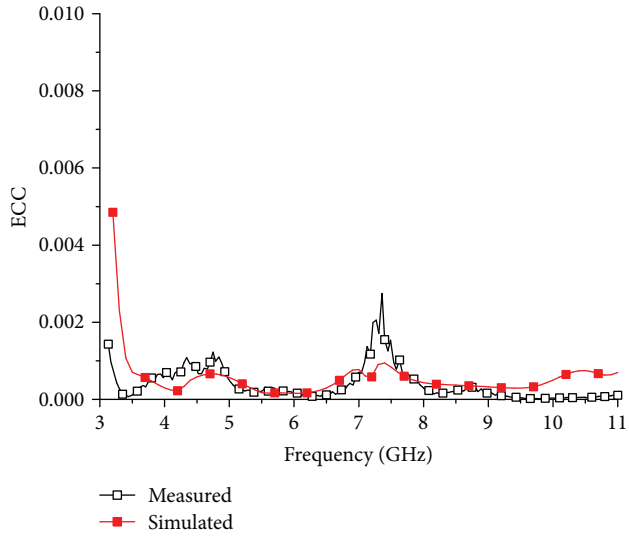

Figure 10: Simulated and measured ECC.

3.2. Radiation Patterns. The simulated and measured 2D radiation patterns at 4 GHz and 10 GHz are shown in Figure 9, when port 1 is excited, the port 2 is terminated with a 50 Ω load and vice versa. Figure 9 shows that the measured data agree with simulated results.

3.3. MIMO Characteristics. The envelope correlation coefficient between the two elements can be calculated using [17].

$$\mathrm{ECC} = \frac{\left|S_{11}^{*}S_{12} + S_{21}^{*}S_{22}\right|^{2}}{\left(1 - \left(\left|S_{11}\right|^{2} + \left|S_{21}\right|^{2}\right)\right)\left(1 - \left(\left|S_{22}\right|^{2} + \left|S_{12}\right|^{2}\right)\right)}. \quad (2)$$

Based on the simulated and measured results, the ECC are calculated and shown in Figure 10. All the values are smaller than 0.005 for the whole UWB band, which guarantees the UWB MIMO antenna has good diversity performance.

4. Conclusions

A novel UWB MIMO antenna has been presented in this paper. Without decoupling structure, high isolation has been achieved by using different types of antenna elements. The UWB MIMO antenna has a compact size and a simple structure. The ground stub between the two antenna elements and the slot line transition were introduced to improve impedance matching of the two elements. Simulation and measurement results show the proposed antenna has an impedance bandwidth that covers the whole UWB band with isolation below −18 dB.

Conflicts of Interest

The authors declare that they have no conflicts of interest.

Acknowledgments

This work is supported in part by the Natural Science Foundation of China under grant 61401106 and in part by the Youth Foundation of Guangdong University of Technology (15ZK0038).

References

[1] T. Kaiser, F. Zheng, and E. Dimitrov, "An overview of ultra-wide-band systems with MIMO," *Proceedings of the IEEE*, vol. 97, no. 2, pp. 285–312, 2009.

[2] G. J. Foschini and M. J. Gans, "On limits of wireless communications in a fading environment when using multiple antennas," *Wireless Personal Communications*, vol. 6, no. 3, pp. 311–335, 1998.

[3] J. F. Li, Q. X. Chu, Z. H. Li, and X. X. Xia, "Compact dual band-notched UWB MIMO antenna with high isolation," *IEEE Transactions on Antennas and Propagation*, vol. 61, no. 9, pp. 4759–4766, 2013.

[4] S. Aqeel, M. H. Jamaluddin, A. Khan et al., "A dual-band multiple input multiple output frequency agile antenna for GPSL1/Wi-Fi/WLAN2400/LTE applications," *International Journal of Antennas and Propagation*, vol. 2016, Article ID 9419183, 11 pages, 2016.

[5] S. Shoaib, I. Shoaib, N. Shoaib, X. Chen, and C. G. Parini, "Design and performance study of a dual-element multiband printed monopole antenna array for MIMO terminals," *IEEE Antennas and Wireless Propagation Letters*, vol. 13, pp. 329–332, 2011.

[6] Z. Yang, H. Yang, and H. Cui, "A compact MIMO antenna with inverted C-shaped ground branches for mobile terminals," *International Journal of Antennas and Propagation*, vol. 2016, Article ID 3080563, 6 pages, 2016.

[7] Y. Wang, J. Yang, S. Hao, and X. Zhang, "Wideband dual-element antenna array for MIMO mobile phone applications," *International Journal of Antennas and Propagation*, vol. 2015, Article ID 434082, 7 pages, 2015.

[8] A. C. K. Mak, C. R. Rowell, and R. D. Murch, "Isolation enhancement between two closely packed antennas," *IEEE Transactions on Antennas and Propagation*, vol. 56, no. 11, pp. 3411–3419, 2008.

[9] S. Zhang, B. K. Lau, A. Sunesson, and S. He, "Closely-packed UWB MIMO/diversity antenna with different patterns and polarizations for USB dongle applications," *IEEE Transactions on Antennas and Propagation*, vol. 60, no. 9, pp. 4372–4380, 2012.

[10] G. Adamiuk, S. Beer, W. Wiesbeck, and T. Zwick, "Dual-orthogonal polarized antenna for UWB-IR technology," *IEEE Antennas and Wireless Propagation Letters*, vol. 8, pp. 981–984, 2009.

[11] L. Liu, H. P. Zhao, T. S. P. See, and Z. N. Chen, "A printed ultra-wideband diversity antenna," in *2006 IEEE International Conference on Ultra-Wideband*, pp. 351–356, Waltham, MA, USA, 2006.

[12] Y. C. Lu and Y. C. Lin, "A compact dual-polarized UWB antenna with high port isolation," in *2010 IEEE Antennas and Propagation Society International Symposium*, Toronto, ON, Canada, 2010.

[13] G. Lin, C. Sung, J. Chen, L. Chen, and M. Houng, "Isolation improvement in UWB MIMO antenna system using carbon black film," *IEEE Antennas and Wireless Propagation Letters*, vol. 16, pp. 222–225, 2016.

[14] K. G. Thomas and M. Sreenivasan, "A simple ultrawideband planar rectangular printed antenna with band dispensation,"

IEEE Transactions on Antennas and Propagation, vol. 58, no. 1, pp. 27–34, 2010.

[15] M. Gopikrishna, D. D. Krishna, C. K. Aanandan, P. Mohanan, and K. Vasudevan, "Compact linear tapered slot antenna for UWB applications," *Electronics Letters*, vol. 44, no. 20, article 1174, 2008.

[16] B. Schupert, "Microstrip/slotline transitions: modeling and experimental investigation," *IEEE Transactions on Microwave Theory and Techniques*, vol. 36, no. 8, pp. 1272–1282, 1988.

[17] S. Blanch, J. Romeu, and I. Corbella, "Exact representation of antenna system diversity performance from input parameter description," *Electronics Letters*, vol. 39, no. 9, p. 705, 2003.